Journal of Metals, Materials and Minerals, 34(1), 1848, 2024

Nano-ZnO prepared by using chaya and mango leaves extract for photocatalyst of methylene blue

Sri Wahyu SUCIYATI[1,2], Junaidi JUNAIDI[2], Rudy SITUMEANG[3], and Posman MANURUNG[2,*]

[1] *Doctoral Program of Mathematics and Natural Science, University of Lampung, Bandar Lampung, 35145, Indonesia*
[2] *Departement of Physics, University of Lampung, Bandar Lampung, 35145, Indonesia*
[3] *Department of Chemistry, University of Lampung, Bandar Lampung, 35145, Indonesia*

***Corresponding author e-mail**: posman.manurung@fmipa.unila.ac.id

Received date:
21 September 2023
Revised date
23 February 2024
Accepted date:
13 March 2024

Keywords:
Nano-ZnO;
Chaya;
Photocatalyst;
Leaves extract

Abstract

This research aimed to synthesize nano-ZnO from chaya (*Cnidoscolus aconitifolius*) and mango leaves extract (*Mangifera indica*) as environmentally friendly photocatalysts. Nano-ZnO was synthesized using green synthesis, with leaves extracts as reducing agents and nanoparticle size stabilizers. The samples were prepared using two methods, namely nano-ZnO-1 and nano-ZnO-2. The results of Fourier transform infrared spectroscopy (FTIR) analysis showed the contribution of metabolite compounds in nano-ZnO synthesis. X-ray diffraction (XRD) and transmission electron microscopy (TEM) showed the crystal size in nano range, with spherical nanorod morphology observed. Ultraviolet-visible diffuse reflectance spectroscopy (UV-Vis DRS) determined the band gap energy of 2.97 eV and 3.17 eV. Furthermore, photocatalytic activity test showed that photocatalyst performance after 90 min was 68.86% (nano-ZnO-1) and 96.46% (nano-ZnO-2).

1. Introduction

Green synthesis is an innovative method of nanomaterial synthesis, using living organisms, such as plants and microorganisms [1]. The use of extracts from these sources can replace the reducing and capping agents from hazardous materials [2] to minimize the toxic effects of chemicals in the metal oxide synthesis process [3]. This method offers several advantages, including biocompatibility [4], cost-effectiveness, simplicity in execution, time efficiency [5-7], and environmental friendliness [8,9]. Among various types of metal oxide often synthesized through green synthesis method is zinc oxide nanoparticles (nano-ZnO), which are particularly used in photo-catalysis [10,11]. Numerous methods have been used for green synthesis of nano-ZnO, including plant-mediated [12,13], green hydrothermal [14], precipitation, and co-precipitation [15].

Water pollution is a significant environmental problem, with organic dyes from the textile industry serving as major pollutants [16]. To remove these pollutants, recent research has used BWOV/CN/CF fabrics for industrial-scale contaminant purification [17]. Another method often used is photocatalysis, which applies metal oxides as oxidizers to degrade organic pollutants. ZnO nanoparticles are metal oxides playing an essential role in photocatalytic degradation and environmental remediation through photocatalysis [18,19], capable of mineralizing harmful organic pollutants from wastewater [20,21]. Nano-ZnO catalyst produced from green synthesis has Methylene Blue (MB) degradation efficiency of approximately 95% [22], reaching 98% [23]. These reports show the exceptional ability of nano-ZnO from plant extract-assisted biosynthesis in degrading organic pollutants. Furthermore, plant extracts containing active compounds function as natural capping and size stabilizers of nano-particles [24].

Green synthesis has been widely used to obtain nano-ZnO with various nanometer scales through leaves extract. Various plant sources include *Hibiscus sabdariffa* [25], *Scadoxus multiflorus* [26], *Mangifera indica* [27], *Aloe vera* [28], *Sesame indicum* [29], *Becium grandiflorum* [30]. This method includes hydrothermal, sol-gel, coprecipitation, and plant-mediated synthesis [31], which require less time consumption, affordable precursors, high product purity, and easy handling procedures with cost-effective equipment [31].

Other plant sources include chaya leaves, which are widely recognized as tree spinach, with numerous health benefits [32,33]. In 100 g chaya leaves, there is abundant phytochemical content including flavonoids (260 mg), saponins (225 mg), carotenoids (190.6 mg), alkaloids (108.3 mg), and phenolics (25.5 GAE) [33,34], serving as a reference for green synthesis of nano-ZnO. The abundance of these metabolites supports the potential of chaya leaves extract as a reducing and capping agent in the green synthesis of nano-ZnO, which has not been carried out. However, the use of mango leaves [27,35], characterized by high phenolic acids, xanthones, benzophenones, tannins, terpenoids, and flavonoids [36] content has been investigated. The application of nano-ZnO synthesized using mango leaves extract [27] in the medical field provides antioxidant activity that is comparable

to standard Vitamin C, although the application in photocatalysis has been reported.

Based on the background above, this research aimed to synthesize nano-ZnO using green synthesis method from chaya (*Cnidoscolus aconitifolius*) and mango leaves extract (*Mangifera indica*) as chelating agents. By using these natural ingredients, zinc nitrate precursor material is anticipated to be effectively modified and functionalized, addressing aggregation issues in nano-ZnO. Furthermore, photocatalytic of nano-ZnO material in degrading MB dye shows effectiveness in reducing organic pollutant molecules.

2. Experimental

2.1 Materials

Materials used included chaya and mango leaves, ethanol (C_2H_6OH) (97%, Merck), sodium hydroxide (NaOH) (75%, Merck), zinc nitrate hexahydrates ($Zn(NO_3)_2.6H_2O$) (95%, Merck), and deionized water. All materials were used without further purification, while ethanol and deionized water were applied for solution neutralization and as the solvent, respectively.

2.2 Methods

2.2.1 Preparation and synthesis of nano-ZnO

Approximately 5 g of both chaya and mango leaves were washed, dried, blended, and added with 100 mL distilled water, followed by heating at 80°C. After 1 hour of heating, extract was cooled, filtered, and stored for further use, and nano-ZnO was obtained using a precipitation method. For this purpose, three solutions were prepared to synthesize nano-ZnO through green synthesis method [35] using chaya and mango leaves extract with the material composition, as shown in Table 1.

Synthesis was carried out in a sequential order, where L1 was added L2 while stirring with a magnetic stirrer for 1 h. This was followed by the addition of L3 dropwise and stirred continuously for 3 h until a dark yellow color formed, indicating the formation of nano-ZnO. Subsequently, the solution was stirred for 20 min at 4000 rpm to obtain the precipitate of nano-ZnO, which was washed alternately using ethanol and distilled water with centrifugation. The precipitate was dried at 80°C for 2 h and the product obtained was crushed using an agate mortar. Each product was named nano-ZnO-1 (LE chaya) and nano-ZnO-2 (LE mango).

2.2.2 Photocatalytic activity

Regarding photocatalytic applications, samples were tested for degradation on MB dyes. Photocatalytic activity was tested using Shimadzu Cary 100 Spectrophotometer with a 200 nm to 800 nm wavelength range. The experiment was carried out using MB concentration of 10 ppm (~100 mL), added with photocatalyst (3.5 g), and irradiated using solar light for 90 min at an interval of 30 min. Exposure time was approximately 11.00 AM to 01.00 PM in July 2023, located at Bandar Lampung (-5.36668°N, 105.24403°W).

Photocatalytic recycling research were carried out for 5 cycles, where the sample was exposed to sunlight for 90 min. Subsequently, the reaction was stopped and the solution was centrifuged for catalyst separation. The catalyst was reused in the next run and the same procedure was repeated 5 times.

2.3 Characterization

A total of two nano-ZnO samples were evaluated for chemical, physical, optical properties, and photocatalytic potential in degrading MB. The functional groups of nano-ZnO were observed using Fourier transform infrared spectroscopy (FTIR) from Agilent/FTIR CARY 630. Subsequently, ZnO structure was analyzed by X-ray diffraction (XRD) using a Panalytical XPert Pro diffractometer, operating at 30 kV and 50 mA with CuKα radiation (λ=1.5406 Å) at a step size of 0.02°. Data were recorded in the 2θ = 20° to 80° range with rotation goniometry and the morphology nano-ZnO was analyzed by TEM, using FEI-Tecnai G2 20 S-Twin. Uv-Vis DRS spectrum analysis was carried out using a CARY 100 Shimadzu Spectrophotometer. Characterization of the specific surface area of ZnO NPs based on N_2 absorption at 77K was recorded using Quantachrome Instruments version 11.0. Before characterization, the samples were degassed at 300°C for 4 h.

3. Results and discussion

3.1 Analysis by using FTIR

FTIR spectra of nano-ZnO are shown in Figure 1.

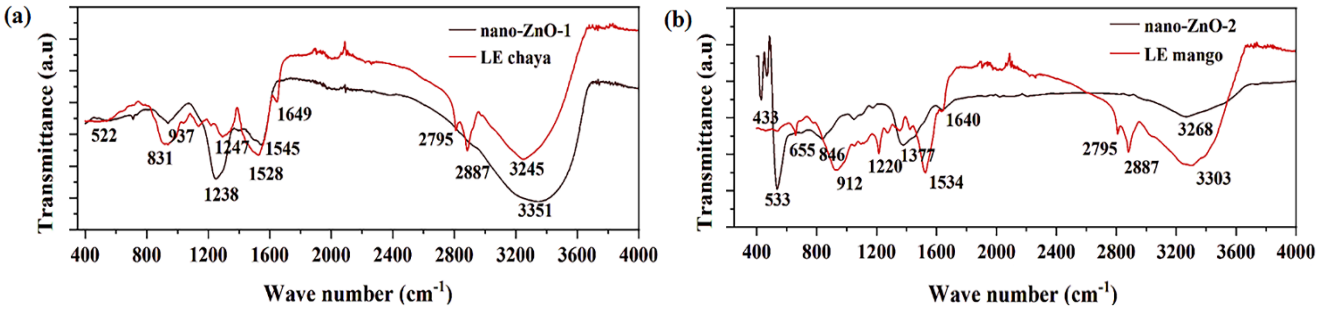

Figure 1. FTIR spectra for: (a) nano-ZnO-1 and LE chaya, (b) nano-ZnO-2 and LE mango.

Table 1. The composition of the solution prepared for chaya and mango samples.

Samples	L1		L2		L3
	$Zn(NO_3)_2.6H_2O$ (M)	Deionized water (mL)	NaOH (M)	Deionized water (mL)	Leaves extract, LE (mL)
(nano-ZnO-1)	1	50	0.7	20	25
(nano-ZnO-2)	0.2	50	0.1	20	25

Table 2. Particle size and structural parameters of the green synthesized nano-ZnO based on Equation (1).

Sample	2θ (°)	B (FWHM) (rad)	Particle size (nm)
nano-ZnO-1	36.288	0.0071	20.4
nano-ZnO-2	36.303	0.0066	22.1

The presence of peaks at 410 through 533 cm^{-1} in all samples showed the characteristics of vibrational of Zn-O bond, indicating zinc oxide [37,38]. Other peaks represented vibration of C=H [10], C-N [37, 39,40], C=O [41], C=C/amine–NH [42,43], and O-H stretching of alcohols and phenols [37,42,43]. According to previous research [43], vibrations of O-H, N-H, and C-O or RCOO were found in LE, associated with alkaloids, flavonoids, and phenolic compounds. This identification showed the presence of flavonoids derivatives in chaya and mango leaves extract. The formation of nano-ZnO could be explained by the linkage of zinc ions (Zn^{2+}) with the functional groups of phyto-chemical compounds, to form a complex $Zn(OH)_4^{2-}$ and grows in strong alkaline solution by adding NaOH. Subsequently, the complex ions were hydrolyzed to form zinc hydroxides, $Zn(OH)_2$, which were altered to Zn^0 by heating or calcining. This process showed the role of chemical compounds in reducing zinc ions [9,44]. FTIR analysis explained the role of organic molecules in LE (chaya and mango) to stabilize the synthesized nano-ZnO. Similarly, nano-ZnO formation occurred due to the interaction of oxygen in the functional groups in LE with zinc molecules in the precursor.

3.2 Analysis of nano-ZnO structure based on XRD patterns

Figure 2 shows XRD diffractogram of nano-ZnO synthesized through green synthesis method from LE, namely *Cnidoscolus aconitifolius* (nano-ZnO-1) and *Mangifera indica* (nano-ZnO-2). The diffraction peaks are positioned with the formation of the hexagonal structure, space group P63MC (186), shown by peak at 2θ corresponding to the standard ZnO database (PDF 01-089-0510). Based on the results, the peaks show various diffraction angles 31.8°, 34.5°, 36.3°, 47.6°, 56.6°, 62.9°, 66.5°, 67.9°, 69.1°, 72.5°, and 77.08°, with the respective Miller's planes (100), (002), (101), (102), (110), (103), (200), (112), (201), (004), and (202). These peaks show ZnO crystalline phase, which is highly intense and narrow, corresponding to the standard database with ZnO samples without impurities. In Figure 2, there is a zinc phosphide phase (PDF 00-053-0591) in nano-ZnO-1. This phase occurs due to a reaction between zinc nitrate precursor and phosphorus content (39 mg/100 g) in chaya leaves [45]. Meanwhile, nano-ZnO-2 has a squaric acid phase (PDF 00-032-1653) and a graphite phase (PDF 01-075-2078). These phases were identified through qualitative analysis by matching experimental data with COD in HighScore Plus software version 3.0.5 using the search match method.

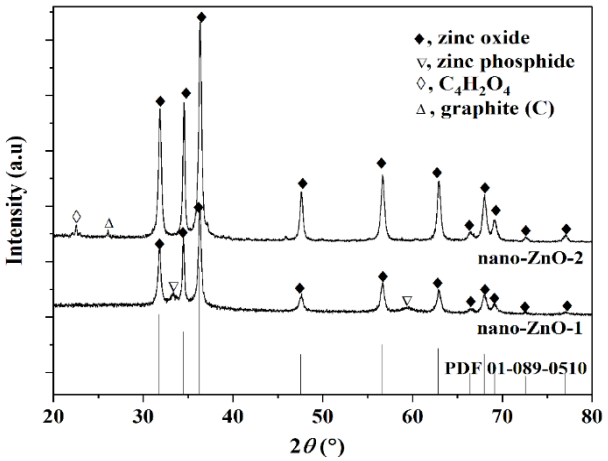

Figure 2. XRD pattern of zinc nanoparticles synthesized from leaves extract of *Cnidoscolus aconitifolius* (nano-ZnO-1) and *Mangifera indica* (nano-ZnO-2). λ = 1.5406Å.

The crystallinity level of nano-ZnO-2 is higher compared to nano-ZnO-1. The smaller concentrations of zinc nitrate and sodium hydroxide in nano-ZnO-2 are not very significant in the growth and formation of ZnO crystals. This phenomenon is attributed to the effect of mango leaves extract, containing richer phytochemical compounds than chaya leaves [35]. The particle size and volume of the hexagonal structure can be calculated using the Scherrer Equation (Equation (1)) [46]:

$$D = \frac{0.9\,\lambda}{B\cos\theta} \quad (1)$$

where D: particle size (nm), λ: X-ray wavelength (1.5406 Å), B: FWHM (rad), θ: diffraction angle (°). By using the data of the highest peak of XRD, the average particle size value for the two ZnO samples is shown in Table 2.

Cell parameters were calculated and analyzed quantitatively using the Rietveld method with Reatica software. The model data used for ZnO (PDF 01-089-0510) was based on data reported by Sawada *et al*. [47] added with a database model from the qualitative analysis. The results presented in Figure 3 showed that the output file had a typical profile for XRD data fitting. The suitability of model data with XRD generally uses a least squares approach, characterized by decreasing the R_B factor and Goodness of Fit (GoF) [48]. In this research, the acceptable R_B suitable parameters and fit goodness

were <1.5 and <1.8, respectively. Based on quantitative analysis, it is known that the molar percentage of nano-ZnO-1 is 97.74%, while nano-ZnO-2 is 98.49%. The refinement results show the zincite lattice parameters in nano-ZnO-1: a = b ≠ c with values a = b = 3.2209 Å and c = 5.2194 Å. In nano-ZnO-2, the values of a = b = 3.2240 Å and c = 5.2003 Å. The parameter values $\alpha = \beta \neq \gamma$ for both nano-ZnO are 90° and 120°.

3.3 TEM micrograph analysis

The morphology of nano-ZnO-1 and nano-ZnO-2 was observed through micrograph images (TEM) with a scale bar of 50 nm, as shown in Figure 4. The formed structure morphology was predominantly nano-spherical with non-uniform size distribution (Figure 4(a)) and appeared as nanorods (Figure 4(b)) with irregular arrangements. This figure showed dispersed nano-ZnO in a semi-spherical shape, while nanorod appeared to cluster, forming black zones due to overlapping and intersection [49], as also reported by Gowthambabu *et al*. [50].

In addition to the overlap between particles, the presence of black zones confirmed Zn with different stoichiometric ratios [51]. TEM images showed average diameter distribution values of 17 nm (nano-ZnO-1) and 21 nm (nano-ZnO-2), which were very close to the calculated XRD data and values obtained by previous research [35]. Selected area electron diffraction (SAED) patterns showed the higher crystallinity of nano-ZnO-2 compared to nano-ZnO-1, confirming the polycrystalline nature of both nano-ZnO.

3.4 The specific surface area of nano-ZnO

Brunauer–Emmett–Teller (BET) analysis of the N_2 adsorption-desorption isotherm in Figure 5 was used to determine the total surface area of both ZnO. Based on the results, nano-ZnO-1 (33.09 $m^2 \cdot g^{-1}$) showed higher total surface area than nano-ZnO-2 (20.81 $m^2 \cdot g^{-1}$) due to low crystal density. The mass of each sample is 0.0475 (nano-ZnO-1) and 0.08029 (nano-ZnO-2). Based on this value, the total specific surface area for the two nano-ZnO is 696.74 $m^2 \cdot g^{-1}$ and 259.49 $m^2 \cdot g^{-1}$. The hysteresis loop in Figure 5 shows the characteristics of type IV adsorption which explains the capillarity phenomenon in mesopores.

3.5 Characterization optical spectra

The optical properties of nano-ZnO-1 and nano-ZnO-2 were observed. The data from the reflectance spectrum were used to estimate the energy bandgap value through the relationship statedby the Tauc plot [52], which was represented as Equation (2):

$$(\alpha h\upsilon)^n = A\left(h\upsilon - E_g\right) \quad (2)$$

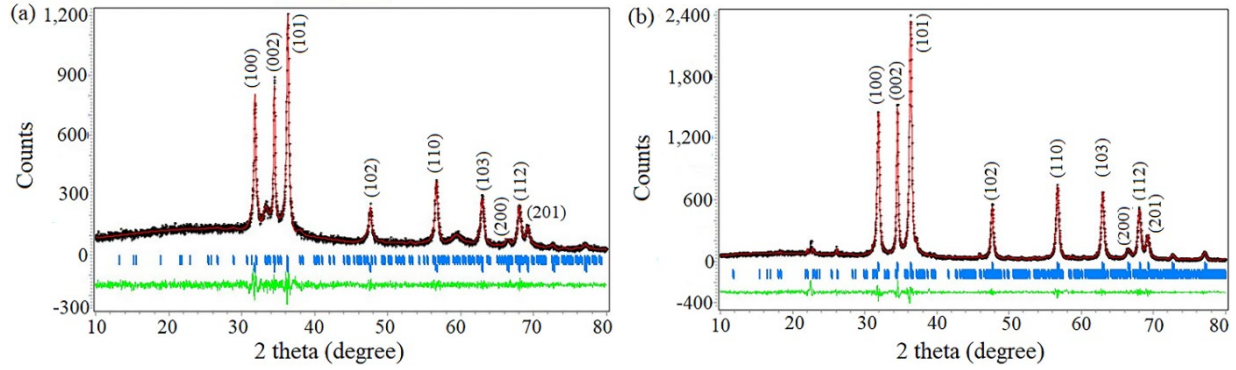

Figure 3. XRD plot for sample: nano-ZnO-1 (a) and nano-ZnO-2 (b). The crossed lines and solid lines indicate the measured and calculated patterns, respectively. λ = 1.5406 Å.

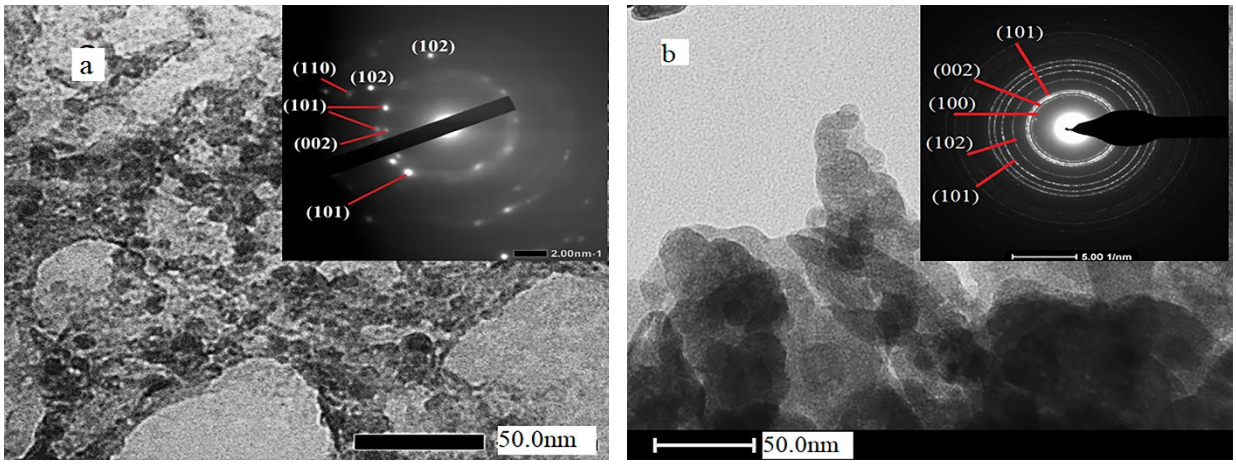

Figure 4. TEM micrographs of nano-ZnO synthesized using Green synthesis method: (a) nano-ZnO-1, and (b) nano-ZnO-2. Bar scale=50 nm.

where *h, A, v, Eg*, are Plank's constant (J s), proportionality constant (J), frequency (Hz), and gap energy (eV), respectively. UV-Visible absorption spectrum was recorded at a wavelength range of 200 nm to 800 nm. Figure 6 shows the optical band gap (*Eg*) of the synthesized nano-ZnO, which was obtained from Equation (2).

The result shows that peak excitonic values of nano-ZnO-1 and nano-ZnO-2 in UV-Vis DRS are 330 nm. This value is smaller compared to excitonic wavelength of bulk ZnO at 388 nm. Absorption peak determines the width of the electron transition between the conduction and the valence band. Generally, absorption peak detected at a particular value can be associated with the reduction of the crystallite structure to nano-size and a quantum confinement effect in the synthesized nano-ZnO [53]. Small peaks between 330 nm to 380 nm and a back-like peak at >400 nm are shown by impurities in the green synthesized nano-ZnO-1. This impurity was detected through XRD diffractogram, as shown in Figure 2, in the presence of zinc phosphide phase. A similar spectrum was also found in previous research [45,54], where the influence of impurity on the appearance of absorption peak was approximately 350 nm to 380 nm.

Based on Equation (2) and Tauc plotting, the band energy gap (*Eg*) was determined to be 2.97 eV (nano-ZnO-1) and 3.17 eV (nano-ZnO-1). This band gap energy showed the wavelength of light effectively absorbed by photocatalyst material. Moreover, a smaller wavelength spectrum width corresponds to a higher energy of photons carried by the radiation. This energy is required to break chemical bonds and initiate photocatalytic reactions. Regarding light absorption, *Eg*=3.17 eV (nano-ZnO-2) will be more efficient in absorbing UV light because it has enough energy to absorb UV light and break specific chemical bonds. However, *Eg*=2.97 eV (nano-ZnO-1) is less effective in absorbing UV light but more effective in transferring electrons from the conduction band to the valence band due to the relatively small energy required for electron transfer. Previous research also showed that the width of *Eg* is influenced by crystallite size, morphology, and synthesis method of nano-ZnO [49,55]. The observed bandgap energies showed that nano-ZnO-1 and nano-ZnO-2 were suitable as photocatalytic materials primarily for absorption of UV light [56-58].

3.6 Photocatalytic activity of nano-ZnO

Testing of photodegradation activity was carried out using MB solution, where the spectrum of blank MB showed peak at 663 nm. Generally, the removal of solution color by photocatalyst usually occurs through photoexcitation process on ZnO surface, leading to the formation of electron-hole pairs on the catalyst surface [59]. Figure 7 shows photodegradation activity of MB dyes (10 ppm) by nano-ZnO-1 and nano-ZnO-2 photocatalysts.

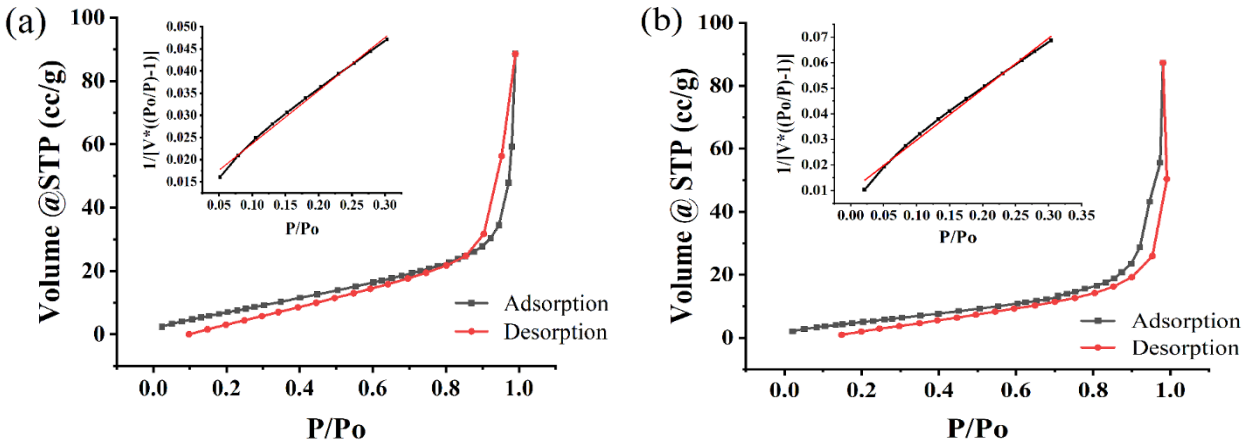

Figure 5. N2 adsorption-desorption isotherm and SBET (insert), (a) nano-ZnO-1 and (b) nano-ZnO-2.

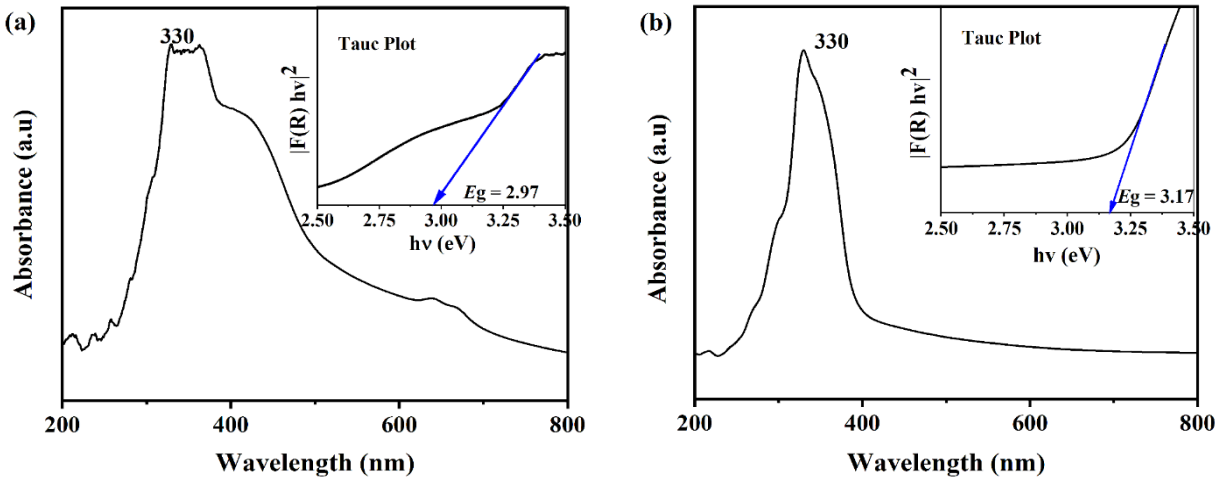

Figure 6. UV-Vis DRS absorption spectra versus wavelength, and Tauc plots (insert) for nano-ZnO-1 (a) and nano-ZnO-2 (b).

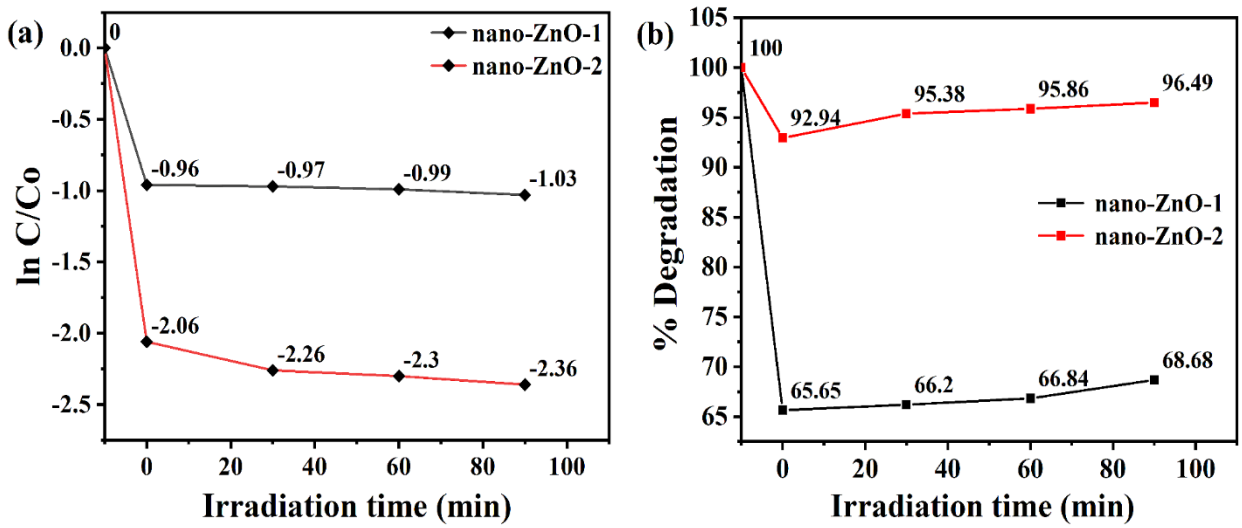

Figure 7. (a) The reaction kinetics, and (b) efficiency of degradation MB color by nano-ZnO-1 and nano-ZnO-2 catalysts.

Photocatalyst activity is interpreted through analysis of photocatalytic data, particularly on the reaction kinetics calculated using pseudo-first-order kinetic equation (Equation (3)). The efficiency of the degradation of MB molecule is calculated by Equation (4) [60]:

$$ln\frac{C}{C_0} = -kt \quad (3)$$

$$\%\ \text{Degradation} = \left(\frac{A_0-A}{A_0}\right) \times 100\% \quad (4)$$

where C, C_0, k, t, A_0, and A, represent MB concentration after adsorption, initial MB concentration, reaction rate constant, exposure time, initial adsorption without photocatalyst, and photocatalyst adsorption, respectively.

Based on Equation (3), the reaction rate of nano-ZnO-1 is calculated to be 0.0008 ppm·min^{-1}, which is smaller than nano-ZnO-2 at 0.0954 ppm·min^{-1}, showing a slower degradation of MB color by nano-ZnO-1. In addition to the band gap width, the particle size affects photocatalytic efficiency. Specifically, Dnano-ZnO-1 < Dnano-ZnO-2 influences the surface area of nano-ZnO-1 to be smaller than nano-ZnO-2, which reduces the number of active sites available to adsorb substrate molecules. This phenomenon shows that MB dye degradation is slowed due to the limited number of simultaneous reactions. Previous research [61,62] stated that surface profile influenced photoactivity of photocatalytic materials. Furthermore, reduction and oxidation reactions on nano-ZnO surface produce electrons and holes, which interact with oxygen (O_2) and water molecules to form superoxide radicals (O^{2-}) and hydroxyl (OH•) [23]. These reactive ions facilitate the process of deactivating and breaking down contaminants or other organic compounds into small molecules through photocatalyst, induced by light/photons [60].

The efficiency of reducing MB dye concentration, as calculated using Equation (4), is 68.86% and 96.49% for nano-ZnO-1 and nano-ZnO-2, respectively. This shows that nano-ZnO-2 is very effective in reducing MB dyes, which is 27.81% faster than nano-ZnO-1. As shown in Figure 2, the high crystallinity of nano-ZnO-2 is attributed to MB degradation performance [63]. The recycling of photocatalyst is presented in Figure 8, showing a decrease in photocatalytic efficiency with each reuse. In this research, photocatalyst was recycled five times, with an efficiency reduction of 8.6% (nano-ZnO-2) and 10.65% (nano-ZnO-1) due to the accumulation of pollutant particles on photocatalyst surface.

The green synthesis carried out by Narath *et al*. [23] and Algarni *et al*. [64] using LE of *Cinnamomum tamala* and LE of *Rosmarinus officinalis* degraded MB by 98.07% (90 min) and 96.7% (90 min). Compared to this research, chaya and mango leaves extract as chelating agents of green synthesis of nanoZnO-1 and nano-ZnO-2 successfully degraded MB, although with degradation efficiencies of 68.86 and 96.49% for 90 min. Specifically for mango leaves extract, the efficiency of the resulting photocatalyst (nano-ZnO-2) is close to *Cinnamommum tamala* leaves extract [23]. This result showed that the calcination temperature after green synthesis process from 500°C to 700°C was a crucial factor contributing to the high MB degradation efficiency of nano-ZnO. However, green synthesis carried out using LE chaya and LE mango obtained efficiency of approximately 68.86% (90 min) and 96.49% (90 min). The synthesis process used a temperature of approximately 80°C for sample drying without calcination. Although the temperature was relatively low, green synthesis method used successfully obtained nano-ZnO with performance as photocatalyst.

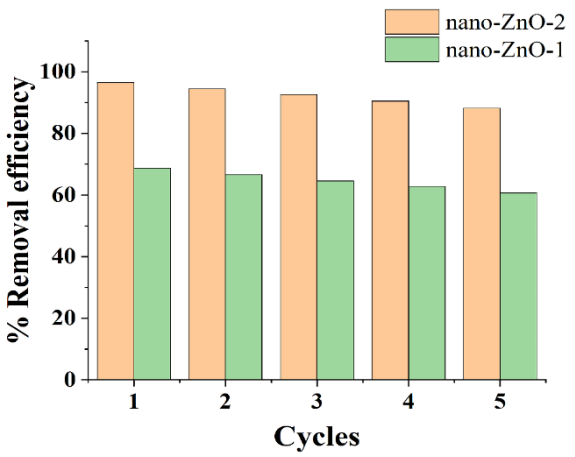

Figure 8. Recycling test for photocatalyst reusability.

4. Conclusion

In conclusion, this research successfully synthesized nano-ZnO using leaves extract of *Cnidoscolus aconitifolius* (nano-ZnO-1) and *Mangifera indica* (nano-ZnO-2) at 80°C. The results of FTIR spectra showed the presence of metabolite compounds included in the formation of nanoparticles. TEM and XRD analyses confirmed the spherical and rod-like morphology as well as the hexagonal wurtzite structure of the synthesized nano-ZnO. The strong absorption peak was detected at 330 nm by UV-Vis DRS. Furthermore, photocatalytic tests showed that nano-ZnO-2 was more efficient in photodegradation of MB dye compared to nano-ZnO-1. Based on kinetic research, the method of photodegradation followed pseudo-first-order kinetics and was dependent on dye concentration. The crystal structure of nano-ZnO, such as particle size and bandgap energies, showed potential effect on photocatalytic activity of nano-ZnO synthesized. This research also showed that particle size and crystallinity played an essential role, indicating high MB degradation efficiency of nano-ZnO-2.

Acknowledgements

With great gratitude to the Institute for Research and Community Service, Lampung University, which supported this research and funded it through the Basic Research scheme with contract number 728/UN26.21/PN/2023.

References

[1] H. Agarwal, S. Venkat Kumar, and S. Rajeshkumar, "A review on green synthesis of zinc oxide nanoparticles – An eco-friendly approach," *Resource-Efficient Technologies*, vol. 3, pp. 406-413, 2017.

[2] J. Jeevanandam, S. F. Kiew, S. Boakye-Ansah, S. Y. Lau, A. Barhoum, M. K. Danquah, J. Rodrigues, "Green approaches for the synthesis of metal and metal oxide nanoparticles using microbial and plant extracts," *Nanoscale*, vol. 14, pp. 2534-2571, 2022.

[3] O. V. Kharissova, B. I. Kharisov, C. M. O. González, Y. P. Méndez, and I. López, "Greener synthesis of chemical compounds and materials," *Royal Society Open Science*, vol. 6, no. 11, p. 191378, 2019.

[4] J. Iqbal, B. A. Abbasi, T. Yaseen, S. A. Zahra, A. Shahbaz, S. A. Shah, S. Uddin, X. Ma, B. Raouf, S. Kanwal, W. Amin, T. Mahmood, H. A. El-Serehy, and P. Ahmad, "Green synthesis of zinc oxide nanoparticles using Elaeagnus angustifolia L. leaf extracts and their multiple in vitro biological applications," *Scientific Reports,* vol. 11, pp. 1-13, 2021.

[5] J. Duraimurugan, G. S. Kumar, P. Maadeswaran, S. Shanavas, P. M. Anbarasan, and V. Vasudevan, "Structural, optical and photocatlytic properties of zinc oxide nanoparticles obtained by simple plant extract mediated synthesis," *Journal of Materials Science: Materials in Electronics*, vol. 30, pp. 1927-1935, 2019.

[6] Y. Xu, J. Jin, X. Li, Y. Han, H. Meng, T. Wang, X. Zhang, "Simple synthesis of ZnO nanoflowers and its photocatalytic performances toward the photodegradation of metamitron," *Materials Research Bulletin*, vol. 76, pp. 235-239, 2016.

[7] S. T. Fardood, F. Moradnia, A. H. Ghalaichi, S. Danesh Pajouh, and M. Heidari, "Facile green synthesis and characterization of zinc oxide nanoparticles using tragacanth gel: investigation of their photocatalytic performance for dye degradation under visible light irradiation," *Nanochemistry Research*, vol. 5, pp. 69-76, 2020.

[8] R. Chandran and A. Mallik, "Facile, seedless and surfactant-free synthesis of ZnO nanostructures by wet chemical bath method and their characterization," *Applied Nanoscience*, vol. 8, pp. 1823-1830, 2018.

[9] H. Chemingui, T. Missaoui, J. C. Mzali, T. Yildiz, M. Konyar, M. Smiri, N. Saidi, A. Hafiane, and H. C. Yatmaz, "Facile green synthesis of zinc oxide nanoparticles (ZnO NPs): Antibacterial and photocatalytic activities," *Materials Research Express*, vol. 6, p. 1050b4, 2019.

[10] R. Vinayagam, S. Pai, G. Murugesan, T. Varadavenkatesan, and R. Selvaraj, "Synthesis of photocatalytic zinc oxide nanoflowers using Peltophorum pterocarpum pod extract and their characterization," *Applied Nanoscience*, vol. 13, pp. 847-857, 2021.

[11] U. Wijesinghe, G. Thiripuranathar, F. Menaa, H. Iqbal, A. Razzaq, and H. Almukhlifi, "Green synthesis, structural characterization and photocatalytic applications of ZnO nano-conjugates using Heliotropium indicum," *Catalysts*, vol. 11, p. 0831, 2021.

[12] V. N. Kalpana and V. Devi Rajeswari, "A review on green synthesis, biomedical applications, and toxicity studies of ZnO NPs," *Bioinorganic Chemistry and Applications*, vol. 2018, pp. 1-12, 2018.

[13] C. Vidya, C. Manjunatha, M. Sudeep, S. Ashoka, and M. A. Lourdu Antony Raj, "Photo-assisted mineralisation of titan yellow dye using ZnO nanorods synthesised via environmental benign route," *SN Applied Sciences*, vol. 2, pp. 1-15, 2020.

[14] M. G. Batterjee, A. Nabi, M. R. Kamli, K. A. Alzahrani, E. Y. Danish, and M. A. Malik, "Green hydrothermal synthesis of zinc oxide nanoparticles for uv-light-induced photocatalytic degradation of ciprofloxacin antibiotic in an aqueous environment," *Catalysts*, vol. 12, pp. 1-17, 2022.

[15] M. A. Tănase, M. Marinescu, P. Oancea, A. Răducan, C. I. Mihaescu, E. Alexandrescu, C. L. Nistor, L. I. Jinga, L. M. Ditu, C. Petcu, and L. O. Cinteza, "Antibacterial and photocatalytic properties of ZnO nanoparticles obtained from chemical versus Saponaria officinalis extract-mediated synthesis," *Molecules*, vol. 26, 2021.

[16] J. Gangwar and J. K. Sebastian, "Unlocking the potential of biosynthesized zinc oxide nanoparticles for degradation of synthetic organic dyes as wastewater pollutants," *Water Science Technology*, vol. 84, pp. 3286-3310, 2021.

[17] M. Cai, Y. Liu, K. Dong, X. Chen, and S. Li, "Floatable S-scheme Bi_2WO_6/C_3N_4/ carbon fiber cloth composite photocatalyst for efficient water decontamination," *Chinese Journal of Catalysis*, vol. 52, pp. 239-251, 2023.

[18] A. Singh, N. B. Singh, S. Afzal, T. Singh, and I. Hussain, "Zinc oxide nanoparticles: a review of their biological synthesis, antimicrobial activity, uptake, translocation and biotransformation in plants," *Journal of Materials Science*, vol. 53, pp. 185-201, 2018.

[19] P. Raizada, A. Sudhaik, and P. Singh, "Photocatalytic water decontamination using graphene and ZnO coupled photocatalysts: A review," *Materials Science for Energy Technologies*, vol. 2, pp. 509-525, 2019.

[20] L. V Bora, and R. K. Mewada, "TiO_2 and ZnO as Heterogeneous Photocatalysts for Wastewater Treatment," *Irjet*, vol. 3, pp. 1610-1616, 2016.

[21] M. Golmohammadi, M. Honarmand, and S. Ghanbari, "A green approach to synthesis of ZnO nanoparticles using jujube fruit extract and their application in photocatalytic degradation of organic dyes," *Spectrochimica Acta - Part A: Molecular and Biomolecular Spectroscopy*, vol. 229, p. 117961, 2020.

[22] S. Pai, S. H, T. Varadavenkatesan, R. Vinayagam, and R. Selvaraj, "Photocatalytic zinc oxide nanoparticles synthesis using Peltophorum pterocarpum leaf extract and their characterization," *Optik*, vol. 185, pp. 248-255, 2019.

[23] S. Narath, S. K. Koroth, S. S. Shankar, B. George, V. Mutta, S. Waclawek, M. Černík, V. V. T. Padil, and R. S. Varma, "Cinnamomum tamala leaf extract stabilized zinc oxide nanoparticles: A promising photocatalyst for methylene blue degradation," *Nanomaterials*, vol. 11, 2021.

[24] H. Veisi, S. Azizi, and P. Mohammadi, "Green synthesis of the silver nanoparticles mediated by Thymbra spicata extract and its application as a heterogeneous and recyclable nanocatalyst for catalytic reduction of a variety of dyes in water," *Journal of Cleaner Production*, vol. 170, pp. 1536-1543, 2018.

[25] C. A. Soto-Robles, P. A. Luque, C. M. Gómez-Gutiérrez, O. Nava, A. R. Vilchis-Nestor, E. Lugo-Medina, R. Ranjithkumar, and A. Castro-Beltrán, "Study on the effect of the concentration of Hibiscus sabdariffa extract on the green synthesis of ZnO nanoparticles," *Results in Physics*, vol. 15, p. 102807, 2019.

[26] N. A. Al-Dhabi and M. V. Arasu, "Environmentally-friendly green approach for the production of zinc oxide nanoparticles and their anti-fungal, ovicidal, and larvicidal properties," *Nanomaterials*, vol. 8, 2018.

[27] S. Rajeshkumar, S. V. Kumar, A. Ramaiah, H. Agarwal, T. Lakshmi, and S. M. Roopan, "Biosynthesis of zinc oxide nanoparticles usingMangifera indica leaves and evaluation of their antioxidant and cytotoxic properties in lung cancer (A549) cells," *Enzyme and Microbial Technology*, vol. 117, pp. 91-95, 2018.

[28] N. I. Rasli, H. Basri, and Z. Harun, "Zinc oxide from aloe vera extract: two-level factorial screening of biosynthesis parameters," *Heliyon*, vol. 6, p. e03156, 2020.

[29] S. Zafar, A. Ashraf, M. U. Ijaz, S. Mauzammil, M. H. Siddique, S. Afzal, R. Andleeb, K. A. Al-Ghanim, F. Al-Misned, Z. Ahmed, and S. Mahboob, "Eco-friendly synthesis of antibacterial zinc nanoparticles using Sesamum indicum L. extract," *Journal of King Saud University - Science*, vol. 32, pp. 1116-1122, 2020.

[30] M. H. Kahsay, "Synthesis and characterization of ZnO nanoparticles using aqueous extract of *Becium grandiflorum* for antimicrobial activity and adsorption of methylene blue," *Applied Water Science*, vol. 11, pp. 1-12, 2021.

[31] S. Bognár, P. Putnik, and D. Š. Merkulov, "Sustainable green nanotechnologies for innovative purifications of water: Synthesis of the nanoparticles from renewable sources," *Nanomaterials*, vol. 12, 2022.

[32] L. G. Eduardo, J. M. C. Francisco, J. Q. V. Fernanda, Q. R. David, C. F. Maribel, and G. N. P. Maria, "Effects of the combination of Cnidoscolus aconitifolius and Metformin on the glycemia in streptozotocin-induced diabetes rats," *Journal of Diabetes Endocrinology*, vol. 10, pp. 30-35, 2019.

[33] K. U. Osuocha, A. V Iwueke, and E. C. Chukwu, "Phytochemical profiling, body weight effect and anti-hypercholesterolemia potentials of Cnidoscolus aconitifolius leaf extracts in male albino rat," *Journal of Pharmacognosy and Phytherapy*, vol. 12, pp. 19-27, 2020.

[34] O. B. John and O. A. Opeyemi, "Effect of processing methods on nutritional composition, phytochemicals, and anti-nutrient properties of chaya leaf (Cnidoscolus aconitifolius)," *African Journal of Food Science*, vol. 9, pp. 560-565, 2015.

[35] M. J. Sierra, A. P. Herrera, and K. A. Ojeda, "Synthesis of zinc oxide nanoparticles from mango and soursop leaf extracts," *Contemporary Engineering Sciences*, vol. 11, pp. 395-403, 2018.

[36] M. Kumar, V. Saurabh, M. Tomar, M. Hasan, S. Changan, M. Sasi, C. Maheshwari, U. Prajapati, S. Singh, R. K. Prajapat, S. Dhumal, S. Punia, R. Amarowicz, and M. Mekhemar, "Mango (*Mangifera indica* L.) leaves: Nutritional composition, phytochemical profile, and health-promoting bioactivities," *Antioxidants*, vol. 10, pp. 1-23, 2021.

[37] A. Hussain, M. Oves, M. F. Alajmi, I. Hussain, S. Amir, J. Ahmed, Md. T. Rehman, and H. R. El-Seedi, I. Ali, "Biogenesis of ZnO nanoparticles using: Pandanus odorifer leaf extract: Anticancer and antimicrobial activities," *Royal Society of Chemistry Advances*, vol. 9, pp. 15357-15369, 2019

[38] E. D. Mohamed Isa, K. Shameli, H. J. Ch'ng, N. W. Che Jusoh, and R. Hazan, "Photocatalytic degradation of selected pharmaceuticals using green fabricated zinc oxide nanoparticles," *Advanced Powder Technology*, vol. 32, pp. 2398-2409, 2021.

[39] S. V. Saraswathi, J. Tatsugi, P. K. Shin, and K. Santhakumar, "Facile biosynthesis, characterization, and solar assisted photocatalytic effect of ZnO nanoparticles mediated by leaves of L. speciosa," *Journal of Photochemistry Photobiology B: Biology*, vol. 167, pp. 89-98, 2017.

[40] P. C. Nagajyothi, S. J. Cha, I. J. Yang, T. V. M. Sreekanth, K. J. Kim, and H. M. Shin, "Antioxidant and anti-inflammatory activities of zinc oxide nanoparticles synthesized using Polygala tenuifolia root extract," *Journal of Photochemistry Photobiology B: Biology*, vol. 146, pp. 10-17, 2015.

[41] R. Rathnasamy, P. Thangasamy, R. Thangamuthu, S. Sampath, and V. Alagan, "Green synthesis of ZnO nanoparticles using Carica papaya leaf extracts for photocatalytic and photovoltaic applications," *Journal of Materials Science: Materials in Electronics*, vol. 28, pp. 10374-10381, 2017.

[42] M. Gupta, R. S. Tomar, S. Kaushik, R. K. Mishra, and D. Sharma, "Effective antimicrobial activity of green ZnO nano particles of Catharanthus roseus," *Frontiers in Microbiology*, vol. 9, pp. 1-13, 2018.

[43] S. Alamdari, M. S. Ghamsari, C. Lee, W. Han, H. Park, M.J. Tafreshi, and H. Afarideh, "Preparation and Characterization

of Zinc Oxide Nanoparticles Using Leaf Extract of Sambucus ebulus," *Applied Sciences*, vol. 10, pp. 1-19, 2020.

[44] P. Basnet, T. Inakhunbi Chanu, D. Samanta, and S. Chatterjee, "A review on bio-synthesized zinc oxide nanoparticles using plant extracts as reductants and stabilizing agents," *Journal of Photochemistry and Photobiology B: Biology*, vol. 183, pp. 201-221, 2018.

[45] A. Garcia, Kuri, J.L. Chavez, "Phenolic profile and antioxidant capacity of Cnidoscolus chayamansa and Cnidoscolus aconitifolius: A review," *Journal of Medicinal Plants Research*, vol. 11, pp. 713-727, 2017.

[46] B. Cullity and S. Stock, *Elements of X-Ray Diffraction*, Third. United States of America: Pearson, 2014.

[47] H. Sawada, R. Wang, and A. W. Sleight, "An electron density residual study of zinc oxide," *Journal of Solid State Chemistry*, vol. 122, pp. 148-150, 1996.

[48] G. Will, *Powder diffraction: The rietveld method and the two stage method to determine and refine crystal structures from powder diffraction data*. Berlin Heidelberg: Springer, 2006.

[49] S. Agarwal, L. K. Jangir, K. S. Rathore, M. Kumar, and K. Awasthi, "Morphology-dependent structural and optical properties of ZnO nanostructures," *Applied Physics A: Materials Science and Processing*, vol. 125, 2019.

[50] V. Gowthambabu, A. Balamurugan, R. Dhivya bharathy, S. Satheeshkumar, and S. S. Kanmani, "ZnO nanoparticles as efficient sunlight driven photocatalyst prepared by solution combustion method involved lime juice as biofuel," *Spectrochimica Acta - Part A: Molecular and Biomolecular Spectroscopy*, vol. 258, p. 119857, 2021.

[51] C. López-Esmerio, C. Ruiz-Rojas, J. Angulo-Rocha, E. Lizárraga-Medina, F. Ramos-Brito, E. Camarillo-García, R. Martinez-Martinez, M. Aguilar-Frutis, and M. García-Hipólito, "Study of the electrical, optical and morphological properties in submicron and microstructured ZnO thin films obtained by spin coating and chemical bath deposition," *Science and Technology Indonesia*, vol. 7, no. 3, p. 291-302, 2022.

[52] J. Tauc and A. Menth, "States in the gap," *Journal of Non-Crystalline Solids*, vol. 8-10, pp. 569-585, 1972.

[53] Y. Gu, I. L. Kuskovsky, M. Yin, S. O'Brien, and G. F. Neumark, "Quantum confinement in ZnO nanorods," *Applied Physics Letters*, vol. 85, pp. 3833-3835, 2004.

[54] P. Devaraji, M. Mapa, H. M. A. Hakkeem, V. Sudhakar, K. Krishnamoorthy, and C. S. Gopinath, "ZnO-ZnS heterojunctions: A potential candidate for optoelectronics applications and mineralization of endocrine disruptors in direct sunlight," *ACS Omega*, vol. 2, pp. 6768-6781, 2017.

[55] Y. Köseoğlu, "A simple microwave-assisted combustion synthesis and structural, optical and magnetic characterization of ZnO nanoplatelets," *Ceramics International*, vol. 40, pp. 4673-4679, 2014.

[56] F. Afifah, A. Tjahjono, A. Ridhova, P. Yuniar, D. Maulida, A. Noviyanto, and D. Aryanto, "Influence of Al and Cu doping on the structure , morphology , and optical properties of ZnO thin film," *Indonesian Journal of Chemistry*, vol. 23, pp. 44-52, 2023.

[57] J. Santhoshkumar, S. V. Kumar, and S. Rajeshkumar, "Synthesis of zinc oxide nanoparticles using plant leaf extract against urinary tract infection pathogen," *Resource-Efficient Technologies*, vol. 3, pp. 459-465, 2017.

[58] S. Mondal, S. R. Bhattacharyya, and P. Mitra, "Effect of Al doping on microstructure and optical band gap of ZnO thin film synthesized by successive ion layer adsorption and reaction," *Pramana - Journal of Physics,* vol. 80, pp. 315-326, 2013.

[59] M. G. Batterjee, A. Nabi, M. R. Kamli, K. A. Alzahrani, E. Y. Danish, and M. A. Malik, "Green hydrothermal synthesis of zinc oxide nanoparticles for UV-light-induced photocatalytic degradation of ciprofloxacin antibiotic in an aqueous environment," *Catalysts*, vol. 12, pp. 1-18, 2022.

[60] M. Satheshkumar, B. Anand, A. Muthuvel, M. Rajarajan, V. Mohana, and A. Sundaramanickam, "Enhanced photocatalytic dye degradation and antibacterial activity of biosynthesized ZnO-NPs using curry leaves extract with coconut water," *Nanotechnology for Environmental Engineering.*, vol. 5, 2020.

[61] M. Aiempanakit, P. Sudjai, K. Singsumphan, S. Laksee, and C. Suwanchawalit, "Brazilein modified zinc oxide nanorods with enhanced visible light-responsive photocatalytic efficiency," *Journal of Metals, Materials and Minerals.* vol. 32, pp. 70-76, 2022.

[62] I. Fatimah, G. Purwiandono, P. W. Citradewi, S. Sagadevan, and W. Oh, "Influencing factors in the synthesis of photoactive nanocomposites of ZnO / SiO_2 -Porous heterostructures from montmorillonite and the study for methyl violet photo-degradation," *Nanomaterials*, vol. 11, p. 3427, 2021.

[63] C. Aiempanakit, T. Phantaporn, and K. Aiempanakit, "Enhanced photocatalytic activity of ZnO nanostructures deposited on mesh through electrochemical deposition and thermal oxidation," *Journal of Metals, Materials and Minerals*, vol. 32, pp. 63-69, 2022.

[64] S. T. Algarni, N. A. Y. Abduh, A. Al Kahtani, and A. Aouissi, "Photocatalytic degradation of some dyes under solar light irradiation using ZnO nanoparticles synthesized from Rosmarinus officinalis extract," *Green Chemistry Letters and Reviews*, vol. 15, pp. 460-473, 2022.